HHS Public Access

Author manuscript

J Mater Chem B Mater Biol Med. Author manuscript; available in PMC 2017 August 21.

Published in final edited form as:

J Mater Chem B Mater Biol Med. 2016 August 21; 4(31): 5289–5298. doi:10.1039/C6TB01154C.

Photocrosslinkable chitosan hydrogels functionalized with the RGD peptide and phosphoserine to enhance osteogenesis

Soyon Kim[a], **Zhong-Kai Cui**[b], **Jiabing Fan**[b], **Armita Fartash**[c], **Tara L. Aghaloo**[c], and **Min Lee**[a,b,*]

[a]Department of Bioengineering, University of California, Los Angeles, USA

[b]Division of Advanced Prosthodontics, University of California, Los Angeles, USA

[c]Division of Diagnostic and Surgical Sciences, University of California, Los Angeles, USA

Abstract

Hydrogels derived from naturally occurring polymers are attractive matrix for tissue engineering. Here, we report a biofunctional hydrogel for specific use in bone regeneration by introducing Arg-Gly-Asp (RGD)-containing cell adhesive motifs and phosphorylated serine residues, which are prevalent in native bone extracellular matrix and known to promote osteogenesis by enhancing cell-matrix interactions and hydroxyapatite nucleation, into photopolymerizable methacrylated glycol chitosan (MeGC). Incorporation of phosphoserine into MeGC hydrogels increased the ability of the hydrogels to nucleate mineral on their surfaces. RGD incorporation enhanced cell-matrix interactions by supporting attachment, spreading, and proliferation of bone marrow stromal cells (BMSCs) encapsulated in the hydrogels. Moreover, co-modification of MeGC hydrogels with RGD and phosphoserine synergistically increased osteogenic differentiation of encapsulated BMSCs *in vitro*. The bone healing capacity of the modified hydrogels was further confirmed in a mouse calvarial defect model. These findings suggest a promising hydrogel platform with a specific microenvironment tailored to promote osteogenesis for clinical bone repair.

Graphical abstract

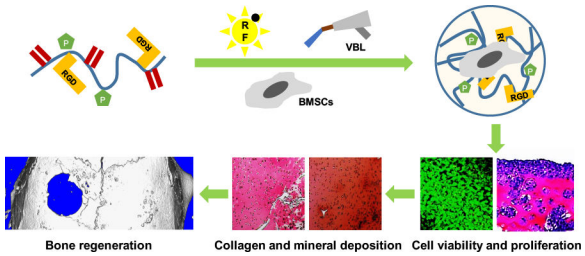

Introduction

Hydrogels derived from naturally occurring polymers are attractive three-dimensional networks for tissue engineering applications due to their high biocompatibility and

*Correspondence - leemin@ucla.edu.

hydrophilicity.[1–3] Moreover, progenitor or stem cells can be delivered into lesions in a minimally invasive manner. Photopolymerization has been widely employed to crosslink hydrogels due to its rapid and mild reactions with minimal cytotoxicity and possible in situ polymerization.[4–12]

We have previously developed a visible blue light (VBL) inducible hydrogel system using methacrylated glycol chitosan (MeGC) and riboflavin (RF, vitamin B2) as a photocrosslinkable polymer and an initiator.[13, 14] In contrast to current photocuring systems using UV light[12, 15], our hydrogel could be prepared under mild conditions, reducing potential adverse effects associated with UV exposure and toxic initiators. Although the hydrogel system supported proliferation and extracellular matrix (ECM) deposition of encapsulated mesenchymal stem cells[16–18], lack of specific cell binding domains on chitosan surfaces and their highly hydrophilic nature with resultant low protein adsorption can limit cell-matrix interactions, leading to poor osteogenic cellular responses[16, 19]. Recently, numerous strategies have been employed to facilitate osteogenesis in hydrogels, including addition of osteogenic growth factors[20] or bioactive filler materials[15, 21], but the hydrogel in itself showed minimal bone forming ability without the additional osteogenic factors or bioactive materials. Thus, there is a need to develop chitosan hydrogel surfaces that present a favorable osteogenic microenvironment.

During osteogenic development, mesenchymal stem cells produce various fibrous ECM proteins such as collagen, in particular, type I collagen, the main structural protein in bone tissue.[15, 22, 23] Type I collagen is known to enhance cellular attachment due to its abundant Arg-Gly-Asp (RGD) residues and to induce osteogenic differentiation.[15, 20, 24–28] In addition, non-collagenous bone ECM proteins such as bone sialoprotein and osteocalcin are known to play an important role in mineral nucleation and osteogenic differentiation.[29] Phosphorylated amino acid residues (e.g. phosphoserine) abundant in such proteins are thought to be responsible for inducing nucleation of hydroxyapatite, resulting in enhance bone formation.[30, 31]

Although the incorporation of collagen in MeGC hydrogels greatly enhanced cellular attachment, proliferation, and osteogenic differentiation of bone marrow stromal cells (BMSCs) in our previous study, use of natural collagen as tissue scaffolds is limited by their potential immune-and pathogenic effects, material variability, and inadequate mechanical strength.[22] As an alternative, numerous studies have focused on the employment of cell adhesion motifs containing RGD to enhance cell-matrix interactions.[26] The incorporation of RGD-containing peptides onto biomaterial surfaces has been shown to enhance cell adhesion and osteogenic differentiation.[32] Moreover, recent studies suggest that phosphoserine is an effective functional group in inducing biomineralization.[33] Surface functionalization with phosphoserine induced highly mineralized matrix that increased osteogenic differentiation and osseointegration on the implant surface.[10, 34]

In this study, we introduce photopolymerizable hydrogel systems functionalized with cell adhesion motifs and phosphorylated groups to enhance osteogenesis (Fig. 1). We hypothesized that incorporation of RGD and phosphoserine to MeGC hydrogels will synergistically enhance osteogenic differentiation of encapsulated cells and bone

regeneration. To test the hypothesis, we will evaluate the ability of the MeGC hydrogels functionalized with RGD peptide and phosphoserine to facilitate mineral nucleation and enhance proliferation and osteogenic differentiation of encapsulated BMSCs. We further investigated the ability of the modified hydrogels to enhance bone formation in a mouse calvarial defect model.

Experimental

Materials

Glycol chitosan (GC, ~100 kDa) was purchased from Wako Chemicals USA, Inc. (Richmond, VA). Glycidyl methacrylate (GMA), O-phospho-L-serine (phosphoserine), 1-ethyl-3-(3-dimethylaminopropyl)-carbodiimide (EDC), tween-20, p-nitrophenol phosphate, β-glycerophosphate, dexamethason, pthalein purple, 8-hydroxyquinolone, 2-amino-2-methyl-1,3-propanedial, alizarin red S and ethylene-diaminetetraacetic acid (EDTA) were supplied from Sigma-Aldrich (St. Louis, MO). Succinimidyl-4-(N-maleimidomethyl) cyclohexane-1-carboxylate (SMCC) was purchased from Pierce (Rockford, IL) and Ac-GCGYGRGDSPG-NH_2 peptide (RGD peptide) was obtained from Anaspec, Inc. (Fremont, CA).

Preparation of photocrosslinkable chitosan hydrogel

2% (w/v) GC in distilled water (DW) was mixed with GMA at 1.1 molar ratio of GMA to the amino groups in GC. The mixture was adjusted to pH 9.0 and located on a shaker at room temperature. After 40 h, the solution was adjusted to pH 7.0 and dialyzed with 50 kDa tubes against with DW for 16 h. The purified solution was lyophilized and rehydrated with 1×phosphate-buffered saline (PBS) to obtain a 2 % (w/v) methacrylated glycol chitosan (MeGC) solution.[4, 18] RGD peptide conjugated photocrosslinkable chitosan (RGD-MeGC) was prepared by SMCC crosslinking reaction. SMCC stock solution was prepared as 7.4 μg/μL in dimethyl sulfoxide (DMSO) and 20 μL of SMCC stock solution was firstly conjugated with 20 mL of 1 % (w/v) MeGC in PBS for 16 h, dialyzed with 50 kDa tubes for 16 h and lyophilized. SMCC conjugated MeGC was rehydrated to 1 % (w/v) in PBS and reacted with 1 mg/mL of RGD peptide in DW for 16 h, dialyzed with 50 kDa tubes for 16 h and lyophilized. Phosphoserine conjugated photo-crosslinkable chitosan (PS-MeGC) was prepared by EDC activated reaction. EDC solution was prepared as 84 mg/mL and 1 mL of EDC solution was reacted with 50 μL of 200 mg/mL phosphoserine in DW for 30 min and mixed with 1 % (w/v) MeGC in PBS for 16 h, dialyzed with 50 kDa tubes for 16 h and lyophilized. Both phosphoserine and RGD peptide conjugated photo-crosslinkable chitosan (PSRGD-MeGC) was prepared by the same method of RGD-MeGC and PS-MeGC preparation. In brief, PS-MeGC was reacted with SMCC and then modified with RGD peptide.

Characterization of hydrogels

The conjugation of RGD peptide and phosphoserine to the MeGC backbone was analyzed via ^1H NMR in D_2O (Bruker ARX400 spectrometer). RGD peptide conjugation was quantified based on the integration of the peaks at 3.8 – 3.9 ppm ($A_{3.8–3.9}$, protons in proline ring in RGD peptide). Phosphoserine conjugation was quantified based on the reduction of

the peaks at 3.4 – 3.7 ppm ($A_{3.4–3.7}$, protons in NH_2). The degree of substitution was reported as relative to total amine groups. The degree of substitution of RGD peptide and phosphoserine was 3.8% and 5.5%, respectively.

The hydrogels were formed by exposing the solution to visible blue light (VBL, 400–500 nm, 300 mW/cm^{-2}, Bisco Inc., Schaumburg, IL) for 80 s in the presence of RF. The incorporation of phosphoserine into photocrosslinkable chitosan hydrogels were characterized by attenuated total reflection-Fourier transform infrared spectroscopy (FTIR, Avatar 360 Thermo Nicolet spectrometer, Thermo Electron Inc., San Jose, CA). MeGC, PS-MeGC and PSRGD-MeGC hydrogels were lyophilized and placed on diamond ATR window and absorbance wavelength spectra were acquired from 4000 to 400 cm^{-1} wavenumbers. Compressive modulus was measured via an indentation experiment by Instron Electro-Mechanical Testing Machines (Instron, Model 5564, Norwood, MA) using a 1.6 mm diameter flat-ended indenter. The compressive modulus was analyzed using a Poissons's ratio of 0.25 as described previously.[13, 16]

Mineral deposition in hydrogels

MeGC, RGD-MeGC, PS-MeGC and PSRGD-MeGC hydrogels were incubated in stimulated body fluid (SBF) for a week. SBF solution was prepared as described previously by sequentially dissolving $CaCl_2$, $MgCl_2$•$6H_2O$, $NaHCO_3$, and K_2HPO_4•$3H_2O$ into DW.[35, 36] The solution was adjusted to pH 6.0 and then Na_2SO_4, KCl, and NaCl were added. The final solution was adjusted to pH 6.5. All hydrogels were fixed in 2.5 % glutaraldehyde (Polysciences, Warrington, PA) for 2 h and imaged using scanning electron microscopy with energy dispersive X-ray microanalysis (SEM-EDS, FEI Nova NanoSEM 230, Hillsboro, OR).

In vitro cell proliferation in hydrogels

The mouse bone marrow stromal cell line (BMSCs, D1 ORL UVA [D1], D1 cell, CRL-12424) was purchased from American Type Culture Collection (ATCC, Manassas, VA). BMSCs were cultured in culture medium (CM) including Low Glucose Dulbecco's Modified Eagle's Medium (DMEM, Life Technologies, Grand Island, NY), 10 % (v/v) Fetal Bovine Serum (FBS, Mediatech Inc, Manassas, VA), 1 % (v/v) Penicillin/Streptomycin (Life Technologies) at 37 °C with 5 % CO_2 humidified atmosphere. BMSCs were trypsinized and encapsulated in hydrogels with 1×10^7 cells/mL concentration. BMSCs encapsulated hydrogels were incubated in CM for 2 weeks and medium was changed twice a week. Cell proliferation was measured by Cell Counting Kit-8 assay (CCK, Dojindo Molecular Technologies, Inc., Kummamoto, Japan). BMSCS in hydrogels were incubated for 3 h in mixed solution of CM and CCK solution as 10 to 1 ratio and color change of media was read at 450 nm. The viability of cells was imaged after calcein/ethidium homodimer staining for 15 min using Live/Dead staining kit (Invitrogen, Carlsbad, CA). BMSCs in hydrogels were imaged under fluorescent microscope. Encapsulated BMSCs in hydrogels were fixed in 10% neutral buffered formalin (NBF) for 16 h, embedded in paraffin and cut into sections of 5 μm thickness. Sectioned slides were deparaffinized and stained with hematoxylin and eosin (H&E) to assess cell proliferation. All the images were obtained with Olympus IX71 microscope (Olympus, Tokyo, Japan).

RNA extraction and quantitative real-time polymerase chain reaction (qRT-PCR)

Hydrogels encapsulated with BMSCs were cultured in osteogenic media (OM) including DMEM, 10 % (v/v) FBS, 1 % (v/v) Penicillin/Streptomycin, 10 mM β-glycerophosphate, 50 μg/mL L-ascorbic acid and 100 nM dexamethasone for 21 days. Samples were collected at day 4 for expression of *Alkaline phosphatase* (*ALP*), *Runx2*, and *Collagen 1a1* (*Col1a*) and day 21 for expression of *Osteocalcin* (*OCN*). Total RNA inside 3D encapsulated samples was extracted using Trizol reagent and RNeasy Mini Plant Kit which were supplied from Qiagen (Valencia, CA). Total isolated RNA (500 ng) was reverse transcribed to cDNA using cDNA transcription kit (Invitrogen). qRT-PCR was carried out in LightCycler 480 PCR system (Indianapolis, IN) with 20 μL SYBR Green. PCR was amplified for 45 cycles and the *GAPDH* expression was used to normalize each gene expression. Primer sequence of each gene was noted as following. *GAPDH*: AGGTCGGTGTGAACGGATTTG (forward), TGTAGACCATGTAGTTGAGGTCA (reverse); *ALP*: GTTGCCAAGCTGGGAAGAACAC (forward), CCCACCCCGCTATTCCAAAC (reverse); *Runx2*: CGGTCTCCTTCCAGGATGGT (forward), GCTTCCGTCAGCGTCAACA (reverse); *Col1a*: AACCCGAGGTATGCTTGATCT (forward), CCAGTTCTTCATTGCATTGC (reverse); *OCN*: GGGAGACAACAGGGAGGAAAC (forward), CAGGCTTCCTGCCAGTACCT (reverse). All the experiments were triplicated.

Osteogenic activity in hydrogels

To induce osteogenic differentiation, BMSCs encapsulated in hydrogels were incubated in OM for 3 weeks and medium was changed twice a week. Samples collected at pre-determined time point were washed with 1×PBS and incubated in a lysis buffer (0.02 % tween-20 in 1×PBS) at 4 °C for 5 min. *p*-Nitrophenol phosphate is used as a substrate to measure ALP activity at an absorbance wavelength of 405 nm. ALP activity was normalized to total protein amount which was determined by Pierce BCA Protein Assay Kit (Thermo Scientific, Rockford, IL). Digested samples were centrifuged and the bottom gel pellets were resuspended in 0.1 N HCl and incubated for overnight at 4 °C. Calcium production was measured by reaction of incubated samples and two buffers. One is 0.024% pthalein purple and 0.25 % 8-hydroxyquinolone in 0.1 N HCl and the other contains 500 mM 2-amino-2-methyl-1,3-propanedial in DW. Reacted samples were read at an absorbance wavelength of 562 nm. BMSCs encapsulated in hydrogels were fixed in 10 % neutral buffered formalin for 16 h and stained with picrosirius red (Polysciences, Inc.) to assess collagen deposition and alizarin red S to assess mineralization. Macroscopic images were taken using Olympus SZX16 Stereomicroscope. For the preparation of histological sections, hydrogel samples were fixed in 10% neutral buffered formalin for 16 h, embedded in paraffin and cut into sections of 5 μm thickness. Sectioned slides were deparaffinized and stained with picrosirius red and alizarin red S. The stained samples were observed with Olympus IX71 microscope was used to obtain images.

Mouse calvarial defect model

All animal procedures were performed in accordance with the Guide for the Care and Use of Laboratory Animals of the University of California, Los Angeles and were approved by the Chancellor's Animal Research Committee. The adult male nude mice (CD-1, 8–12 weeks

old) were purchased from Charles River Laboratories (Wilmington, MA). Adult nude mouse (n = 3–4 per group) was anesthetized and 3 mm diameter critical sized defect was created on calvaria by trephine. Each defect was rinsed with saline solution to remove bone debris and filled with hydrogel solutions containing MSCs followed by VBL irradiation for 40 s. Defect was sutured and closed after all the procedures. All animals were transferred to the vivarium for postoperative care. To prevent potential infection, all animals were subcutaneously injected buprenorphine with a concentration of 0.1 mg/kg for 3 days and received drinking water including trimethoprim-sulfamethoxazole for 7 days.

Three-dimensional micro-computerized tomography scanning

Mice were sacrificed 6 weeks post-surgery and calvaria were collected for further analysis. Calvarial tissues were fixed in 4 % formaldehyde for 48 h at room temperature. Samples were washed and stored in 70 % ethanol solution at 4 °C and imaged under high-resolution microCT (μCT40; Scanco USA, Inc., Southeastern, PA) with 57 kVp, 184 μA, 0.5 mm aluminum filtration and 10 μm resolution. Reconstruction of the microCT data were obtained using Dolphin 3D software (Dolphin Imaging & Management Solutions, Chatsworth, CA). Image J (NIH, Bethesda, Maryland) was used to analyze the size of defect after 6 weeks of healing. Scanned samples were then sent for their corresponding histology.

Histological evaluation

After fixation, calvarial tissues were decalcified in 10 % EDTA solution under gentle shaking for 1 week and solution was replaced once at day 3. Decalcified samples were embedded in paraffin and cut into 5 μm thickness slides. The slides were deparaffinized and stained with H&E, Masson-Goldner Trichrome staining to detect new bone formation. The green color indicated new or mature bone. OCN protein expression was also analyzed by immunohistochemical staining. Deparaffinized sections were incubated with primary antibody against OCN (Santa Cruz Biotechnology Inc., Dallas, TX) and color development was obtained by HRP/DAB detection kit (Abcam, Cambridge, MA).

Statistical analysis

Statistical analysis was performed using one-way analysis of variances (ANOVA), with the Tukey's post hoc test. A value of $p < 0.05$ was considered as significant.

Results

Incorporation of RGD peptide and phosphoserine into hydrogels

Adhesion ligands containing RGD peptide were covalently coupled into MeGC using SMCC crosslinkers and the RGD incorporation were verified with ^{1}H NMR (Fig. 2a). The ^{1}H NMR spectra of RGD-MeGC and PSRGD-MeGC exhibited the appearance of the peaks corresponding to the functional groups contained in the grafted peptide sequence, indicating successful conjugation of RGD peptide. The EDC-activated carboxylic group of phosphoserine was conjugated to the amine group of MeGC and the phosphoserine incorporation was investigated by FTIR (Fig. 2b). The FTIR spectra of PS-MeGC showed the characteristic absorption corresponding to the P=O(OH) group in phosphoserine at 2360 cm^{-1}, indicating successful incorporation of phosphoserine. The mechanical strength of

MeGC hydrogels was characterized by an indentation test. The compressive modulus of MeGC hydrogels was approximately 11.7 kPa and the incorporation of RGD peptide or phosphoserine did not significantly change the mechanical properties of the hydrogels (Fig. 2c).

Mineral deposition in hydrogels

To test the ability of MeGC hydrogels to induce mineral nucleation, hydrogels were incubated in SBF solution and the surface morphology of the hydrogels was observed by SEM (Fig. 3a). Phosphoserine conjugated MeGC hydrogels displayed crystal-like particles on their surfaces after incubation, while smooth hydrogel surfaces were observed with the unmodified hydrogels or MeGC conjugated with RGD peptide only. The composition of the particles deposited on the hydrogels was characterized by EDS analyzer (Fig. 3b). EDS spectra of MeGC hydrogels conjugated with phosphoserine in the absence or presence of RGD peptide revealed high peak intensity of phosphorus (P) element relative to carbon (C) amount approximately 0.043–0.046, which was significantly higher than the groups not containing phosphoserine. The Ca/P ratio of MeGC, RGD-MeGC, PS-MeGC and PSRGD-MeGC was 1.03, 1.08, 1.38 and 1.41, respectively. Increased amount of calcium was also observed on phosphoserine-modified hydrogels.

Cell encapsulation and proliferation in hydrogels

BMSCs encapsulated in hydrogels were round in shape and formed large clusters over the 14-day culture period with no indication of cell spreading (Fig. 4a). Similar cell growth was observed in the hydrogels conjugated with phosphoserine only. In contrast, cells cultured in RGD-modified hydrogels exhibited extensive spreading with a spindle-like shape at day 14. A high level of viability (over 95%) of encapsulated cells was observed in all experimental groups by Live/Dead staining. Proliferation of encapsulated BMSCs in the hydrogels was further investigated by a CCK assay (Fig. 4b). The hydrogels modified with RGD peptide significantly enhanced cell proliferation compared with unmodified hydrogels. The incorporation of phosphoserine did not result in significant differences in cell proliferation over the culture period. Morphology of BMSCs cultured in the hydrogels was observed by histological examination (Fig. 4c). H&E staining exhibited large cell aggregated near the surface of unmodified MeGC hydrogels or hydrogels modified with phosphoserine only at day 14. In contrast, BMSCs cultured in the hydrogels modified with RGD peptide extensively spread with a spindle-like shape and proliferated along the surface of the hydrogel. Moreover, cells in hydrogels co-modified with RGD peptide and phosphoserine formed dense cellular layers near the periphery of the hydrogel and intense cell growth extended toward the center of the hydrogel.

In vitro osteogenic differentiation

The osteogenic gene expression of BMSCs cultured in hydrogels was assessed by qRT-PCR (Fig. 5). The modification of MeGC hydrogels with RGD peptide or phosphoserine significantly increased expression of early osteogenic markers *ALP* and *Col1a* as well as a critical osteogenic regulator *Runx2*, compared with unmodified hydrogels at day 4. Significantly higher expression of *ALP* was observed in BMSCs cultured in hydrogels co-modified with RGD peptide and phosphoserine, compared with groups modified with RGD

peptide or phosphoserine alone. The expression level of OCN was significantly increased in hydrogels modified with RGD peptide or phosphoserine alone, with strong promotion of the gene in groups co-modified with RGD peptide and phosphoserine at day 21.

Osteogenic differentiation of BMSCs in hydrogels was determined biochemically by monitoring ALP activity and calcium production. ALP expression increased in all experimental hydrogels over the initial 14-day culture period (Fig. 6a). However, cells cultured in MeGC hydrogels co-modified with RGD peptide and phosphoserine expressed significantly higher ALP activity than groups modified with RGD peptide or phosphoserine alone. By 21 days, ALP expression decreased and was not significantly different among the hydrogels. Mineralization was determined by quantifying calcium production in the hydrogels (Fig. 6b). At 21 days of culture, extensive amount of calcium production was observed in hydrogels co-modified with RGD peptide and phosphoserine. The extent of collagen deposition and mineralized matrix was confirmed by picrosirius red and alizarin red S staining appeared in MeGC hydrogels modified with RGD peptide or phosphoserine (Fig. 6c and d). Especially, BMSCs cultured in hydrogels co-modified with RGD peptide and phosphoserine exhibited highly intense positive throughout the entirety of the hydrogel, indicating strong collagen deposition and mineralization.

In vivo calvarial bone formation

Efficacy of hydrogels to promote bone formation was evaluated in mouse calvarial defects at 6 weeks. The μCT analysis revealed significantly increased bone formation in the defects treated with MeGC hydrogels modified with RGD peptide and phosphoserine when compared with control (left empty) or defects treated with unmodified MeGC hydrogels (Fig. 7a). The extent of bone formation was determined by quantifying new bone area in the defects (Fig. 7b). Results demonstrated that modified MeGC hydrogels induced significantly greater percentage healing of defects as compared to unmodified hydrogels (53.4 % vs 33.2 %). The blank control groups showed minimal healing of approximately 10 %.

The new bone formation was further confirmed by histological analysis and immunohistochemistry at 6 weeks. H&E and Masson-Goldner Trichrome staining showed formation of osteoid matrix near the edges of defects treated with modified MeGC hydrogels, while blank or MeGC groups exhibited fibrous-like tissue with minimal bone formation (Fig. 8a). Osteogenic differentiation in defects was further confirmed by performing immunohistochemical staining for OCN (Fig. 8b). Highly intensive positive OCN staining was observed in defects treated with modified MeGC hydrogels compared with the blank or MeGC groups.

Discussion

During bone formation, collagenous matrix synthesized by osteoblasts not only served as cell binding surfaces but also associated with acidic non-collagenous proteins to mediate mineral nucleation from surrounding ions. The primary goal of this study is to create pro-osteogenic hydrogel matrix that mimic natural extracellular microenvironment of bone tissue by introducing RGD peptide and phosphoserine into MeGC already developed in our previous study.

RGD peptide and phosphoserine were chemically tethered onto MeGC by common conjugation techniques using SMCC and EDC. Abundant primary amine groups on chitosan backbone allow for the chemical modification with various crosslinkable groups. Successful incorporation of the functional moieties was confirmed by ^{1}H NMR spectra and FTIR. The matrix stiffness and swelling properties can influence cellular behavior in the hydrogels. Modification of MeGC hydrogel with RGD peptide and phosphoserine did not significantly alter the mechanical property and swelling ratio of the hydrogel.

After incubation of hydrogels in SBF solution, SEM observation demonstrated crystal-like formation on the surface of hydrogels modified with phosphoserine indicating mineral nucleation, while smooth surface was observed in unmodified hydrogels or MeGC modified with RGD peptide only. EDS analysis confirmed that the observed crystal-like structure was mainly composed of calcium and phosphorus elements. This indicates that anionic phosphate groups in phosphorylated hydrogels was able to attract calcium and phosphorus from SBF, thereby initiating hydroxyapatite nucleation.[35, 37] No significant difference on Ca/P ratio was observed between RGD-MeGC and PSRGD-MeGC, indicating that the addition of RGD peptide did not affect the phosphoserine-induced mineral deposition. Similar observation of increased mineralization has been reported on the oligo(polyethylene glycol)fumarate hydrogel surface modified with bis(2-(methacryloyloxy)ethyl)phosphate).[37]

Cell-matrix interactions play important roles in cell growth, survival, and differentiation in bone tissue engineering. Although high cell viability was observed in all experimental MeGC hydrogels as shown by Live/Dead staining, BMSCs encapsulated in pure MeGC hydrogels remained round in shape and formed clusters along the hydrogel surface, indicating minimal cell-matrix interaction. In contrast, BMSCs near the periphery of the MeGC hydrogels modified with RGD peptide greatly spread and proliferated over time. This is mostly mediated by binding of the cell surface integrin receptors to RGD motif present on hydrogel networks, allowing cells to attach and proliferate.[38, 39] Morevoer, BMSCs in hydrogels co-modified with RGD peptide and phosphoserine not only spread and proliferate extensively along the hydrogel surface but also penetrated toward the interior of the hydrogels. It is possible that the employed phosphate groups promoted protein adsorption and integrin-matrix interactions on the hydrogel surface, resulting in increased cell proliferation and matrix remodeling as hydrogels degraded by cell-secreted enzymes. Similar cell growth with dense cellular layers was observed on the MeGC hydrogels modified with collagen in our previous study.[22]

MeGC hydrogels functionalized with RGD peptide not only increased cell attachment and proliferation but also upregulated expression of early osteogenic markers such as *ALP* and *Col1a* as well as *Runx2*, a critical osteogenic regulator. The RGD motif present in ECM molecules is known to induce integrin-mediated adhesion and activate osteogenic signaling pathway by upregulating expression of focal adhesion kinase (FAK) and extracellular signal-regulated kinase (ERK).[23, 40] Phosphoserine modification also elevated the expression level of *ALP*, *Col1a* and *Runx2* in BMSCs. This may be due to alter protein adsorption and biomineralization on phosphate-rich hydrogel surfaces that may mediate osteogenic differentiation. In addition, late osteogenic markers such as *OCN* were greatly enhanced in MeGC hydrogels modified with both RGD peptide and phosphoserine compared with

hydrogels with individual treatment, suggesting the synergistic effects were observed in biochemical assays for ALP activity and calcium production. These observations were further confirmed by biochemical staining for collagen production and mineral deposition.

We also demonstrated osteogenic efficacy of our hydrogel systems modified with RGD peptide and phosphoserine in a mouse calvarial defect model already established in our previous studies. The radiographic images showed that the size of the defects treated with unmodified with MeGC was smaller compared with the defects left empty. The observed increase in bone healing may be attributed to osteogenic differentiation of engrafted ASCs with hydrogels because almost no healing was observed in defects treated with MeGC alone without ASCs (data not shown). Although hydrogels modified with RGD peptide or phosphoserine alone increased *in vitro* osteogenic gene expression and mineral deposition compared with unmodified groups, the hydrogels with individual treatment did not lead to significant increase in bone formation in calvarial defects, indicating that the addition of RGD peptide or phosphoserine alone was not enough to accelerate bone formation *in vivo*. Treatment of defects with MeGC modified with RGD peptide and phosphoserine significantly increased bone regeneration, suggesting efficacy of the functional groups incorporated into hydrogels to promote osteogenesis of implanted cells. Overall, functionalization of MeGC hydrogels with RGD peptide and phosphoserine will provide biomaterial systems to localize precursor cells and promote their osteogenic differentiation in the defective area.

Conclusions

We developed injectable biomaterial systems that mimic bone extracellular environment by incorporating cell adhesion motifs and phosphorylated groups to photocrosslinkable chitosan hydrogels for bone regeneration. Introduction of RGD peptide enhanced adhesion and proliferation of cells encapsulated in chitosan hydrogels and phosphoserine induced mineralization of hydrogels. Moreover, co-modification with RGD peptide and phosphoserine synergistically enhanced osteogenesis *in vitro* and bone formation in a calvarial defect model. The present work suggests that our hydrogel system functionalized with RGD peptide and phosphoserine has a great potential as a biomaterial for bone tissue engineering applications.

Acknowledgments

This work was supported by the National Institutes of Health grants R01 AR060213 and R21 DE021819, the International Association for Dental Research, and the Academy of Osseointegration.

Notes and references

1. Park J-B. Medicina Oral Patologia Oral Y Cirugia Bucal. 2011; 16:E115–E118.
2. Yu L, Ding J. Chemical Society Reviews. 2008; 37:1473–1481. [PubMed: 18648673]
3. Van Tomme SR, Storm G, Hennink WE. International Journal of Pharmaceutics. 2008; 355:1–18. [PubMed: 18343058]
4. Junli H, Yaping H, Hyejin P, Bogyu C, Siying H, Chung A, Min L. Acta Biomaterialia. 2012; 8:1730–1738. [PubMed: 22330279]
5. Nguyen KT, West JL. Biomaterials. 2002; 23:4307–4314. [PubMed: 12219820]

6. Censi R, Vermonden T, van Steenbergen MJ, Deschout H, Braeckmans K, De Smedt SC, van Nostrum CF, di Martino P, Hennink WE. Journal of Controlled Release. 2009; 140:230–236. [PubMed: 19527757]
7. Hoshikawa A, Nakayama Y, Matsuda T, Oda H, Nakamura K, Mabuchi K. Tissue Engineering. 2006; 12:2333–2341. [PubMed: 16968173]
8. Ibusuki S, Halbesma GJ, Randolph MA, Redmond RW, Kochevar IE, Gill TJ. Tissue Engineering. 2007; 13:1995–2001. [PubMed: 17518705]
9. Bahney CS, Lujan TJ, Hsu CW, Bottlang M, West JL, Johnstone B. European Cells & Materials. 2011; 22:43–55. [PubMed: 21761391]
10. Anderson SB, Lin C-C, Kuntzler DV, Anseth KS. Biomaterials. 2011; 32:3564–3574. [PubMed: 21334063]
11. Kruger TE, Miller AH, Wang J. Scientific World Journal. 2013
12. Bae MS, Ohe JY, Lee JB, Heo DN, Byun W, Bae H, Kwon YD, Kwon IK. Bone. 2014; 59:189–198. [PubMed: 24291420]
13. Amsden BG, Sukarto A, Knight DK, Shapka SN. Biomacromolecules. 2007; 8:3758–3766. [PubMed: 18031015]
14. Bogyu C, Soyon K, Lin B, Kevin L, Bezouglaia O, Jinku K, Evseenko D, Aghaloo T, Min L. Acta Biomaterialia. 2015; 12:30–41. [PubMed: 25462526]
15. Xavier JR, Thakur T, Desai P, Jaiswal MK, Sears N, Cosgriff-Hernandez E, Kaunas R, Gaharwar AK. ACS Nano. 2015; 9:3109–3118. [PubMed: 25674809]
16. Hu J, Hou Y, Park H, Choi B, Hou S, Chung A, Lee M. Acta Biomater. 2012; 8:1730–1738. [PubMed: 22330279]
17. Choi B, Kim S, Fan J, Kowalski T, Petrigliano F, Evseenko D, Lee M. Biomaterials Science. 2015; 3:742–752. [PubMed: 26222593]
18. Hyejin P, Bogyu C, Junli H, Min L. Acta Biomaterialia. 2013; 9:4779–4786. [PubMed: 22935326]
19. Kim J, Lin B, Kim S, Choi B, Evseenko D, Lee M. Journal of Biological Engineering. 2015; 9
20. Holloway JL, Ma H, Rai R, Burdick JA. J Control Release. 2014; 191:63–70. [PubMed: 24905414]
21. Choi B, Cui Z-K, Kim S, Fan J, Wu BM, Lee M. Journal of Materials Chemistry B. 2015; 3:6448–6455.
22. Arakawa C, Ng R, Tan S, Kim S, Wu B, Lee M. J Tissue Eng Regen Med. 2014
23. Choi B, Kim S, Lin B, Wu BM, Lee M. ACS Appl Mater Interfaces. 2014
24. Fisher LW, Fedarko NS. Connective Tissue Research. 2003; 44:33–40. [PubMed: 12952171]
25. Masi L, Brandi ML, Robey PG, Crescioli C, Calvo JC, Bernabei P, Kerr JM, Yanagishita M. Journal of Bone and Mineral Research. 1995; 10:187–196. [PubMed: 7754798]
26. Visser R, Arrabal PM, Santos-Ruiz L, Fernandez-Barranco R, Becerra J, Cifuentes M. Tissue Engineering Part A. 2014; 20:34–44. [PubMed: 23859077]
27. Schaffner P, Dard MM. Cellular and Molecular Life Sciences. 2003; 60:119–132. [PubMed: 12613662]
28. Porte-Durrieu MC, Guillemot F, Pallu S, Labrugere C, Brouillaud B, Bareille R, Amedee J, Barthe N, Dard M, Baquey C. Biomaterials. 2004; 25:4837–4846. [PubMed: 15120531]
29. Tye CE, Hunter GK, Goldberg HA. Journal of Biological Chemistry. 2005; 280:13487–13492. [PubMed: 15703183]
30. Bala Y, Farlay D, Boivin G. Osteoporosis International. 2013; 24:2153–2166. [PubMed: 23229470]
31. Watson BM, Vo TN, Tatara AM, Shah SR, Scott DW, Engel PS, Mikos AG. Biomaterials. 2015; 67:286–296. [PubMed: 26232878]
32. Kantlehner M, Schaffner P, Finsinger D, Meyer J, Jonczyk A, Diefenbach B, Nies B, Holzemann G, Goodman SL, Kessler H. Chembiochem. 2000; 1:107–114. [PubMed: 11828404]
33. Benoit DSW, Schwartz MP, Durney AR, Anseth KS. Nature Materials. 2008; 7:816–823. [PubMed: 18724374]
34. Gandavarapu NR, Mariner PD, Schwartz MP, Anseth KS. Acta Biomaterialia. 2013; 9:4525–4534. [PubMed: 22982322]

35. Ju-Yeon L, Bogyu C, Wu B, Min L. Biofabrication. 2013; 5 045003 (045009 pp.)-045003 (045009 pp.).
36. Fan J, Im CS, Guo M, Cui Z-K, Fartash A, Kim S, Patel N, Bezouglaia O, Wu BM, Wang C-Y, Aghaloo TL, Lee M. Stem Cells Translational Medicine. 2016; 5:539–551. [PubMed: 26956209]
37. Dadsetan M, Giuliani M, Wanivenhaus F, Runge MB, Charlesworth JE, Yaszemski MJ. Acta Biomaterialia. 2012; 8:1430–1439. [PubMed: 22277774]
38. Baxter LC, Frauchiger V, Textor M, ap Gwynn I, Richards RG. European Cells & Materials. 2002; 4:1–17. [PubMed: 14562250]
39. Lian J. Connective Tissue Research. 1992; 27:135–146.
40. Hamidouche Z, Fromigue O, Ringe J, Haeupl T, Vaudin P, Pages J-C, Srouji S, Livne E, Marie PJ. Proceedings of the National Academy of Sciences of the United States of America. 2009; 106:18587–18591. [PubMed: 19843692]

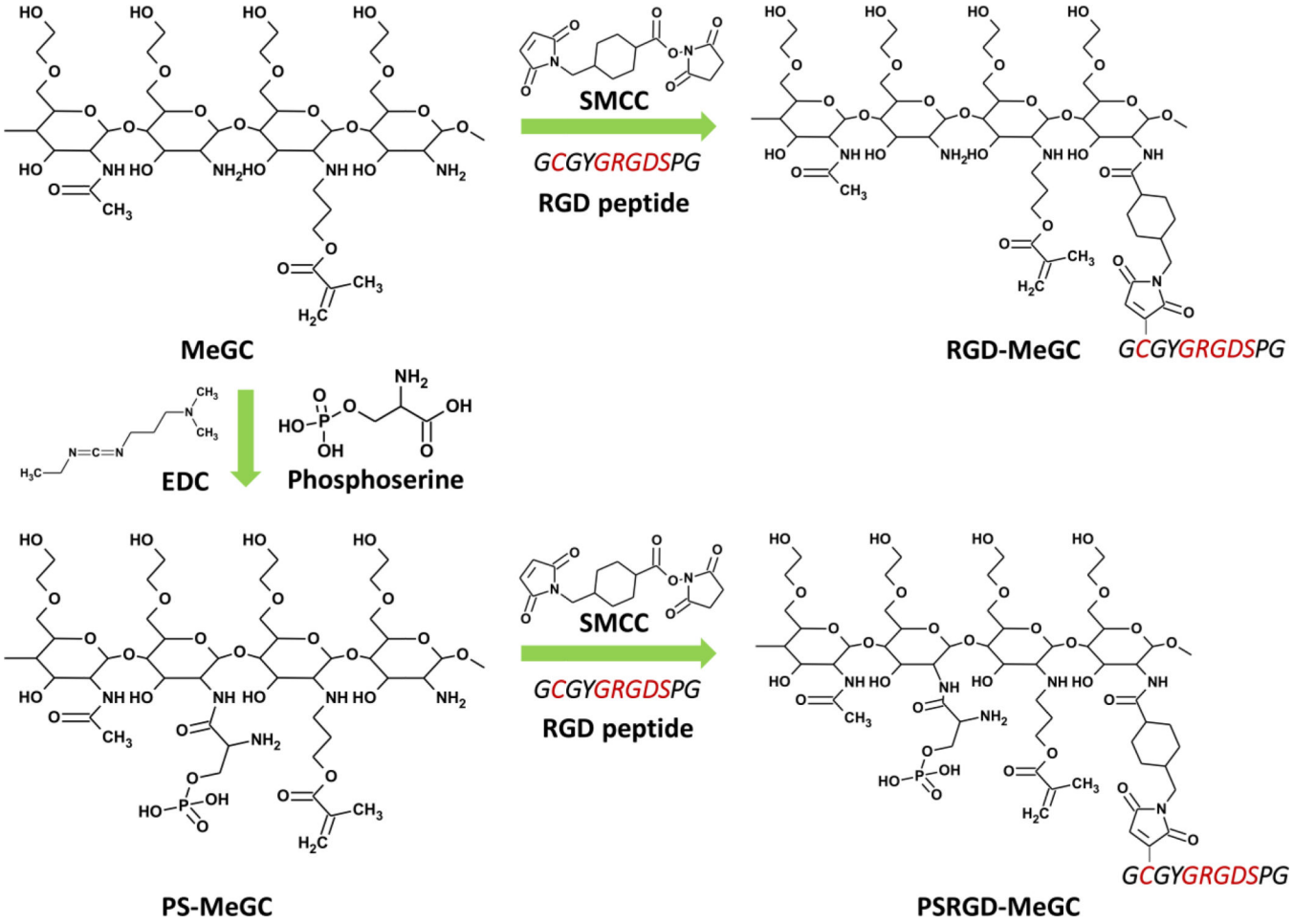

Fig. 1.

Modification of hydrogels with RGD peptide and/or phosphoserine (RGD-MeGC, PS-MeGC and PSRGD-MeGC).

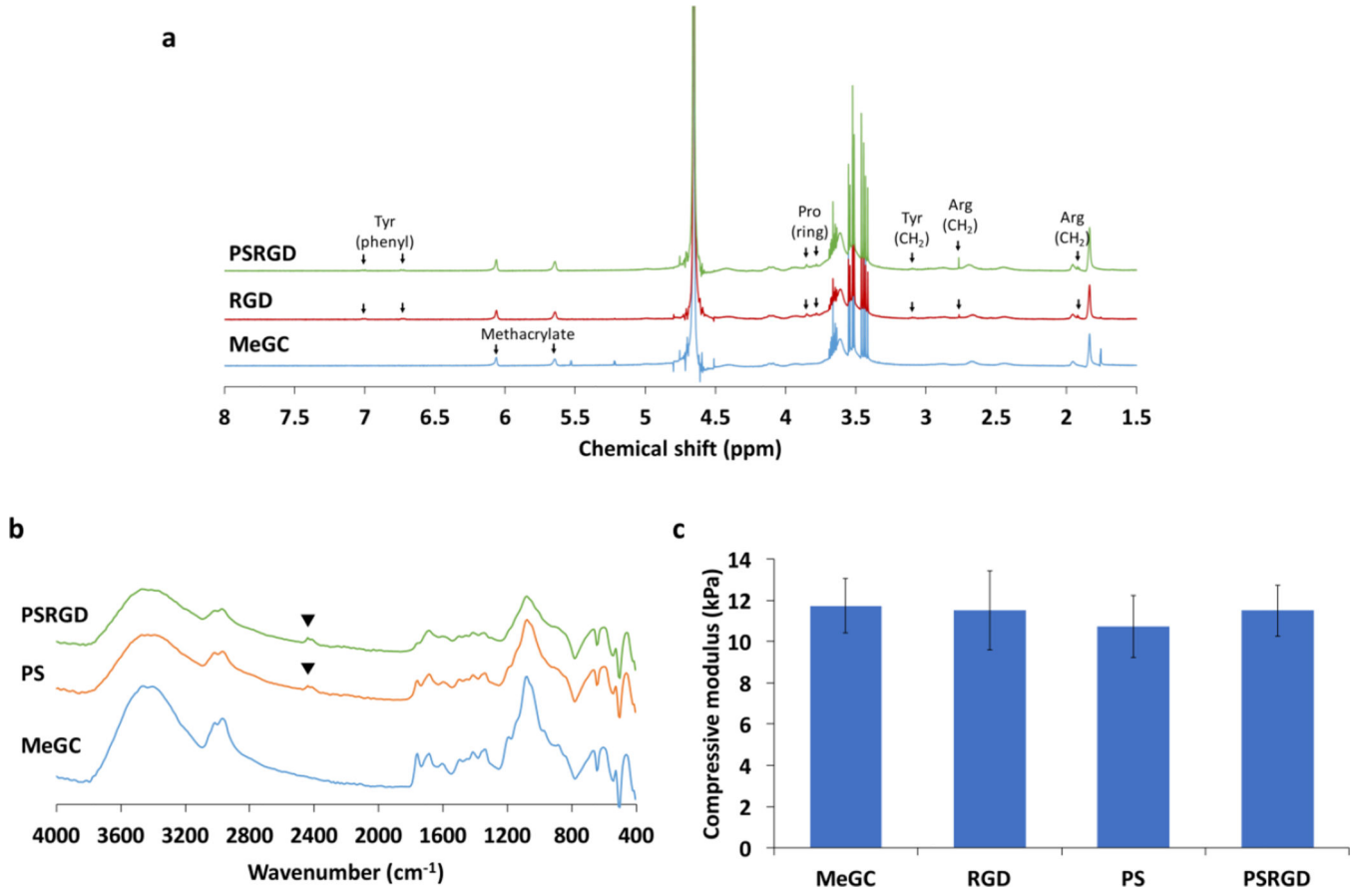

Fig. 2.

Characterization of modified hydrogels. (a) ^{1}H NMR spectra of MeGC, RGD-MeGC and PSRGD-MeGC (400 MHz, D_2O) to analyze conjugation of RGD peptide. (b) FTIR spectra of MeGC, PS-MeGC and PSRGD-MeGC to detect phosphoserine in modified hydrogels. (c) Compressive modulus of MeGC, RGD-MeGC, PS-MeGC and PSRGD-MeGC hydrogels.

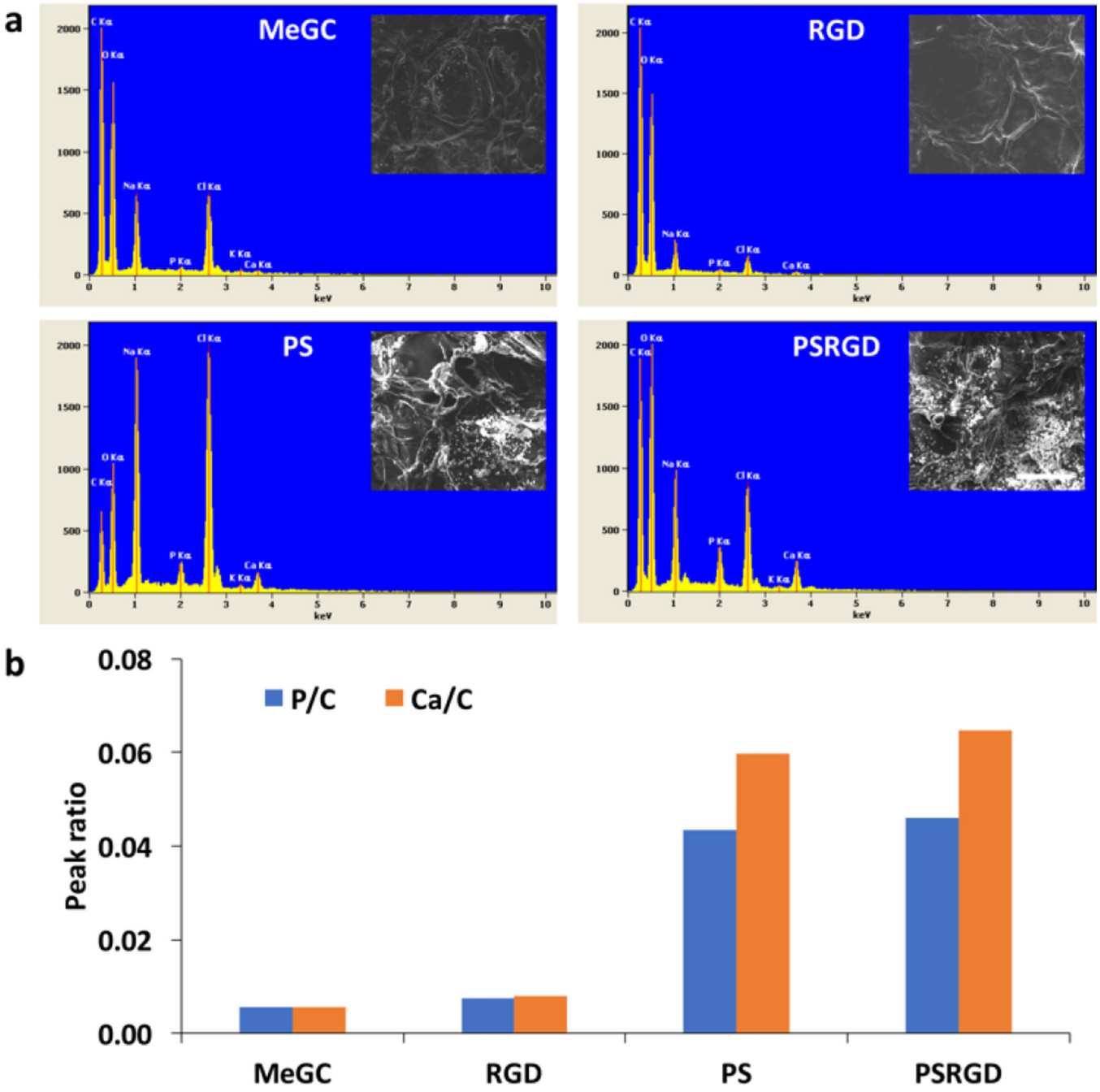

Fig. 3.

Mineral deposition in hydrogels. (a) SEM images and EDS spectra after a week incubation in simulated body fluid (SBF). The scale bar is 100 μm. (b) Characterization of calcium (Ca) and phosphorus (P) peaks on the hydrogel surfaces. The peak intensity of both calcium and phosphorous is normalized to the carbon (c) peak height. The P/C and Ca/C ratio were obtained from are integration analysis.

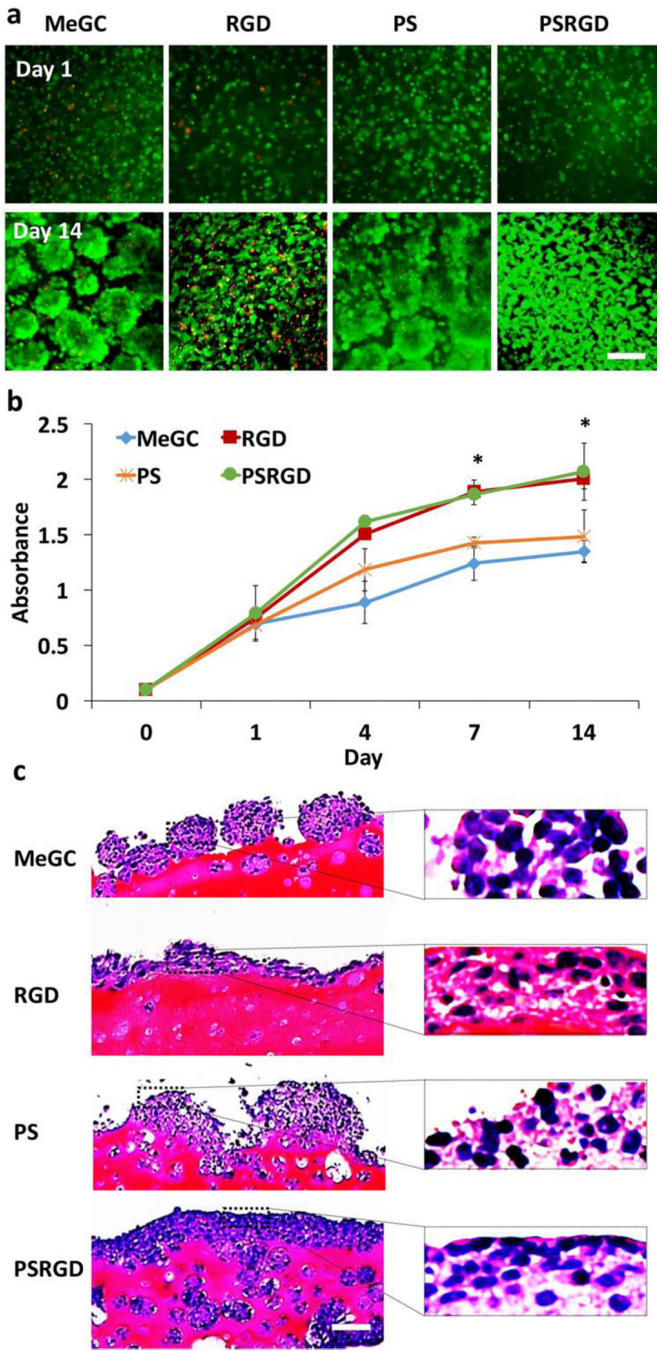

Fig. 4.

Proliferation of BMSCs encapsulated in hydrogels for 2 weeks-culture. (a) BMSCs viability and morphology in hydrogels observed with Live/Dead staining. (b) Proliferation of BMSCs in hydrogels determined by CCK assay (*$p < 0.05$). (c) Histological analysis of BMSCs in hydrogels. The scale bar is 100 μm.

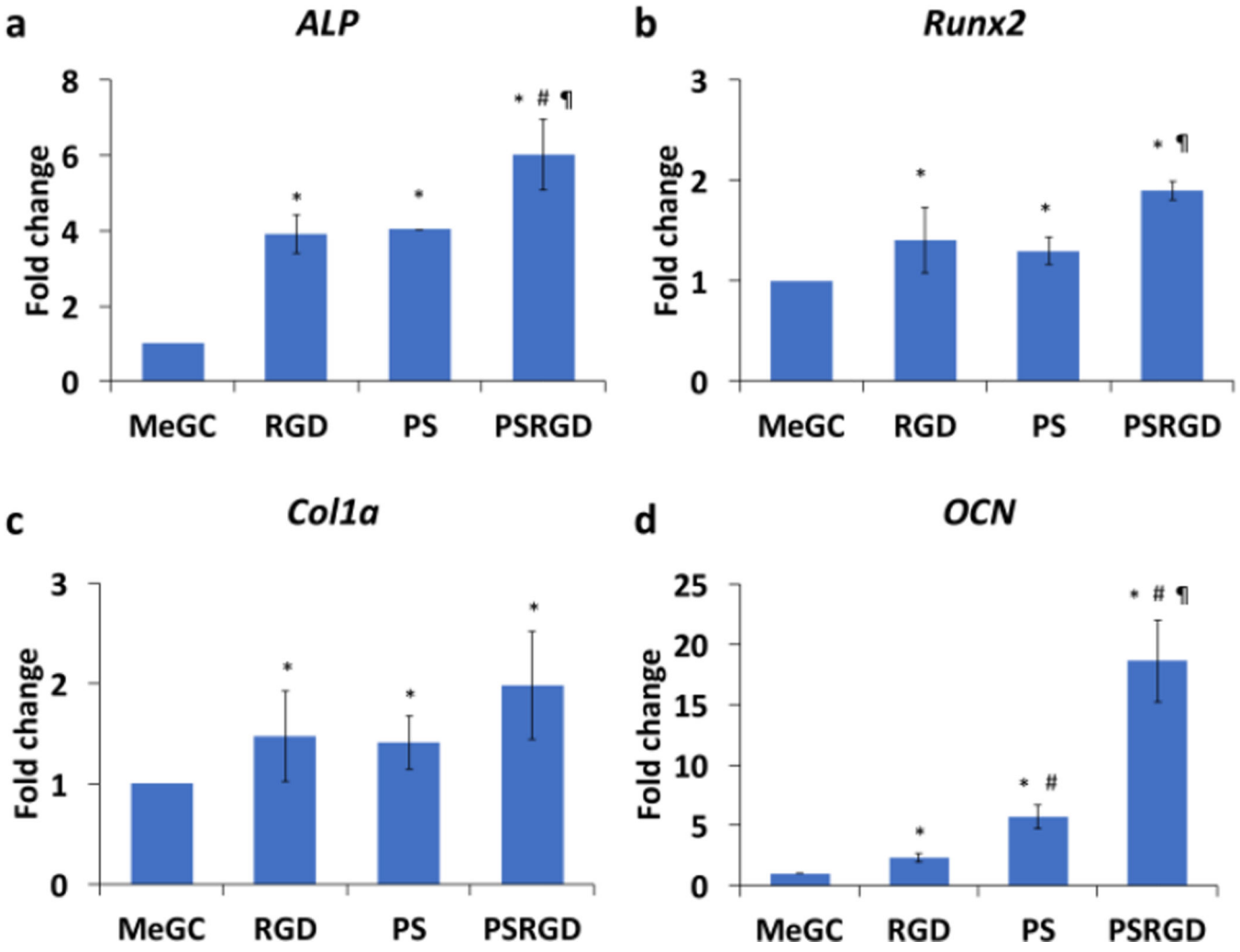

Fig. 5.

Osteogenic gene expression of BMSCs cultured in hydrogels (a) *ALP* (b) *Runx2* (c) *Col1a* and (d) *OCN* expression in hydrogels. (*) compared to MeGC, (#) compared to RGD and (¶) compared to PS ($p < 0.05$)

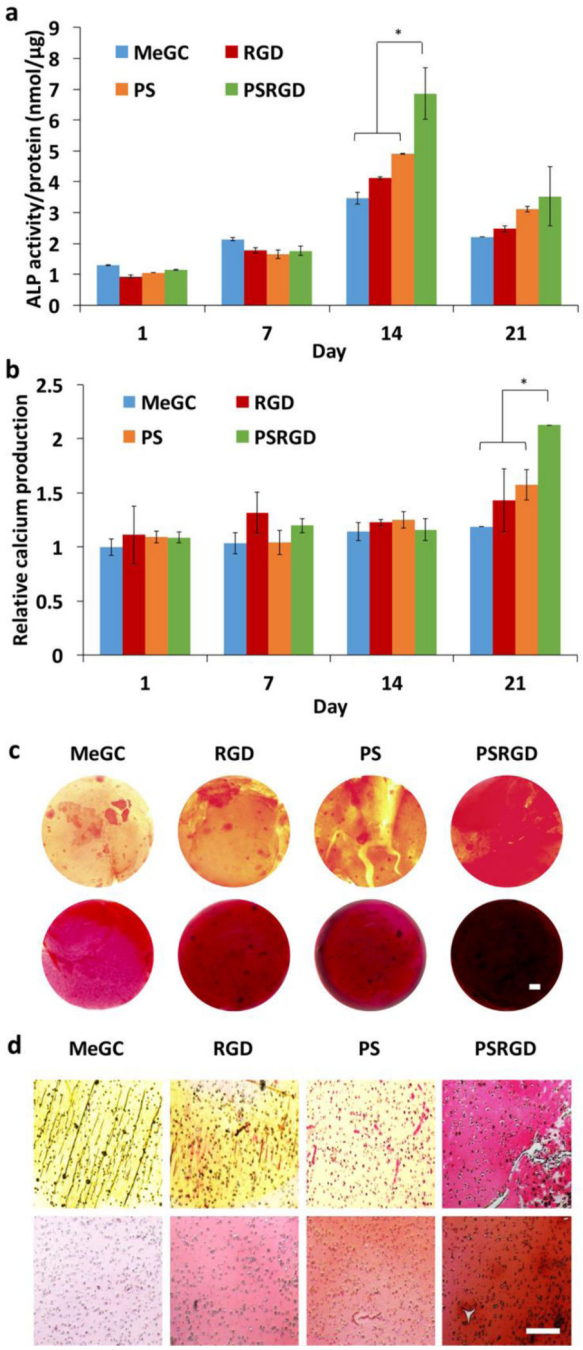

Fig. 6.

In vitro osteogenic differentiation determined by ALP activity, calcium production and histological analysis. (a) ALP activity of BMSCs in hydrogels (*$p < 0.05$). (b) Calcium production of BMSCs in hydrogels (*$p < 0.05$). (c) Picrosirius red (top) and alizarin red S (bottom) staining of hydrogel constructs (d) Picrosirius red (top) and alizarin red S (bottom) staining of hydrogel sections. The scale bar is 100 μm.

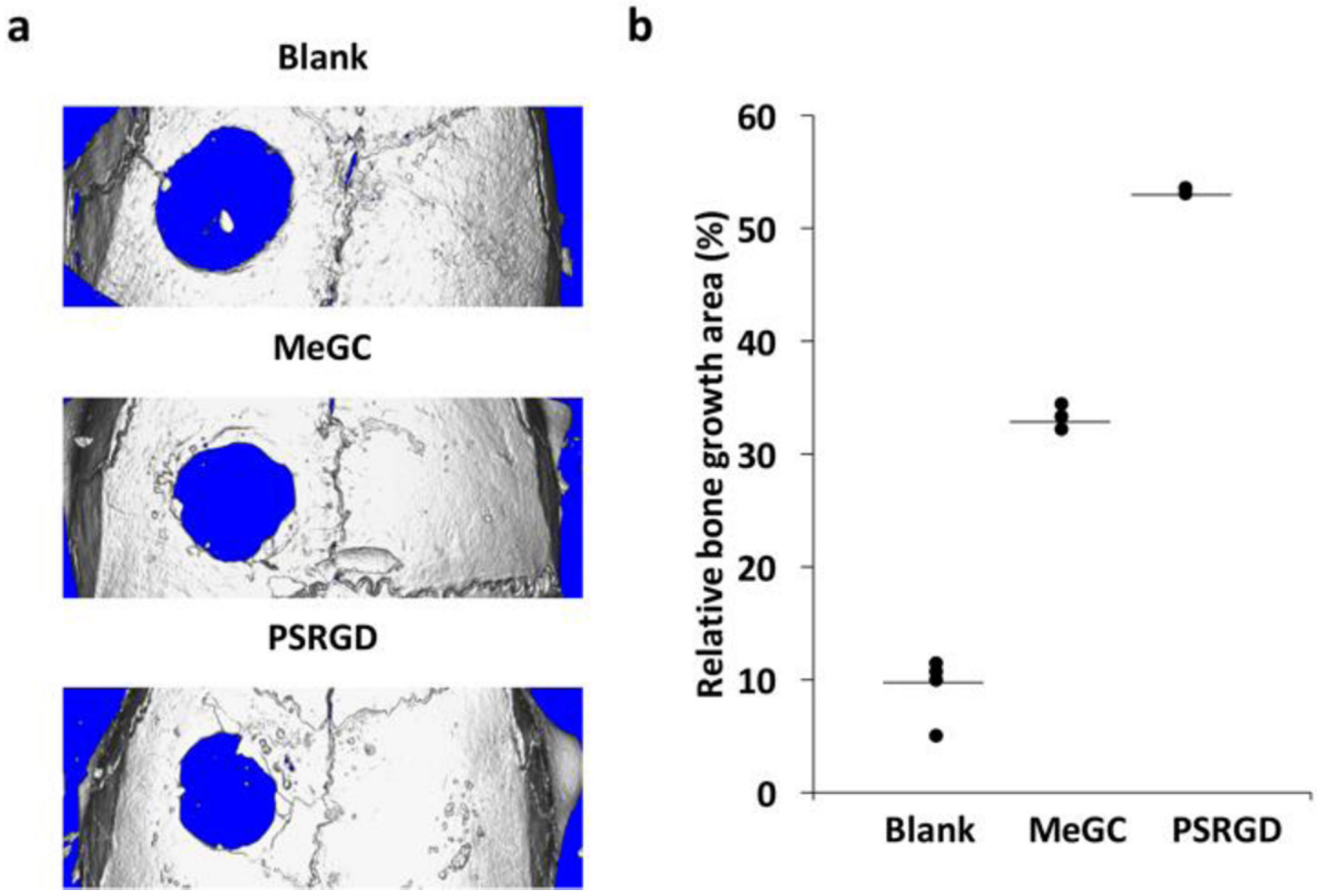

Fig. 7.

In vivo calvarial bone formation. (a) μCT images of calvarial defects treated with hydrogels after 6 weeks. (b) Relative bone growth surface area normalized to the original defect size

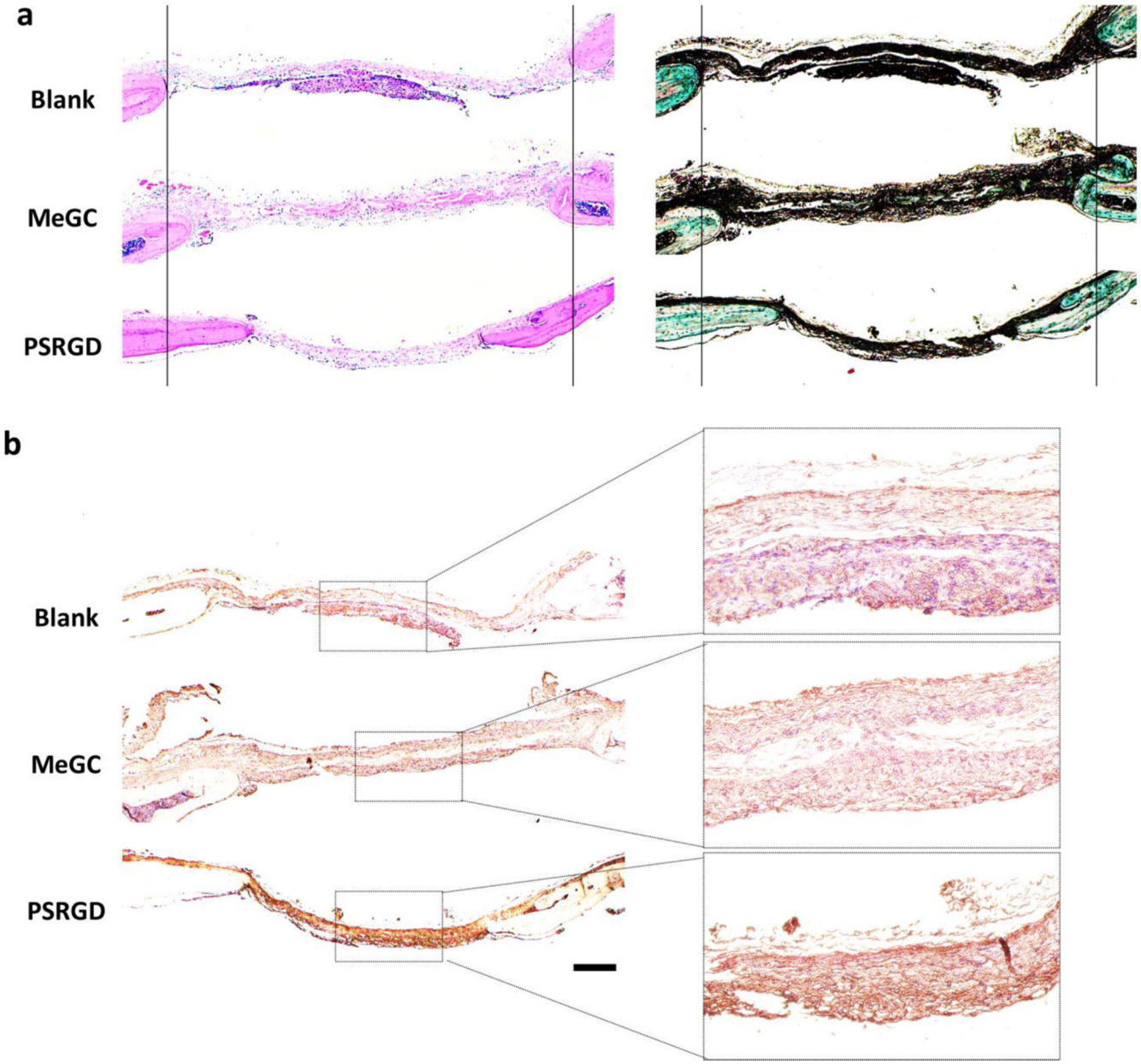

Fig. 8.

Histological evaluation and immunohistochemistry of regenerated bone in calvarial defects. (a) H&E (left) and Masson-Goldner Trichrome (right) staining of calvarial defects. For the ease of observation, two vertical lines were drawn. (b) Immunohistochemical staining of OCN. The scale bar is 200 μm.